Segmentation of Melanoma Skin Lesions Using Anisotropic Diffusion and Adaptive Thresholding

Conference Paper · April 2018

DOI: 10.1145/3208955.3208961

5 authors, including:

Adil Humayun Khan
Prince Mohammad University
13 PUBLICATIONS **27** CITATIONS
SEE PROFILE

Ghazanfar Latif
Prince Mohammad University
47 PUBLICATIONS **129** CITATIONS
SEE PROFILE

Dody Iskandar
Lampung University
13 PUBLICATIONS **16** CITATIONS
SEE PROFILE

Jaafar Alghazo
Prince Mohammad bin fahad University
57 PUBLICATIONS **131** CITATIONS
SEE PROFILE

Segmentation of Melanoma Skin Lesions using Anisotropic Diffusion and Adaptive Thresholding

Adil H. Khan, Ghazanfar Latif
Universiti Malaysia Sarawak, Malaysia.
Prince Mohammad bin Fahd University, Saudi Arabia.
akhan@pmu.edu.sa, glatif@pmu.edu.sa

D.N.F. Awang Iskandar
Universiti Malaysia Sarawak, Malaysia.
dnfaiz@unimas.my

Jaafar Alghazo, Mohsin Butt
Prince Mohammad bin Fahd University, Saudi Arabia.
King Fahd University of Petroleum and Minerals, Saudi Arabia.
jghazo@pmu.edu.sa, mohsinbutt@kfupm.edu.sa

ABSTRACT
Segmentation is the first and most important task in the diagnosis of skin cancer using computer-aided systems and due to complex structure of skin lesions, the automated process may lead to a completely different diagnosis. In this paper, a novel segmentation method of skin lesions is proposed which is both effective and simple to implement. Smoothing of skin lesions in original image plays a pivotal role to secure an accurate segmented image. Anisotropic Diffusion Filter (ADF) is used in the initial stage to smooth images with preserved edges. Adaptive thresholding is then applied to segment the skin lesion of the image by binarizing it. The morphological operations are applied for further enhancement and final segmented image is obtained by applying proposed boundary conditions in which objects are selected on basis of distance. The proposed technique is tested on over 300 images and averaged results are compared with existing methods like L-SRM, Otsu-R, Otsu-RGB and TDLS. The proposed method achieved an average accuracy of 96.6%. Visual results for selected images also depicted better performance of proposed method even in the presence of bad illumination and rough skin lesions in the image.

Keywords
Melanoma Skin Lesions, Segmentation, Anisotropic Diffusion, Skin Cancer, Adaptive Thresholding.

1. INTRODUCTION
Melanoma is a type of skin cancer that originates from small pigments on the skin of subjects. The pigments contain cells that called melanocytes. Fatality rates caused by melanoma skin lesions are the highest amongst skin cancer patients. Melanoma skins cancer has been on the rise for the past few year [1]. The dermatologists need to screen every patient thoroughly for possible infection. Image processing techniques can help the dermatologists by automatically filtering the melanoma affected patients.

A dermatoscope is a device which is used to capture different skin conditions. The device uses a magnifier which is illuminated by a light input which helps in capturing the color and microstructures of skin lesions more accurately. The images obtained from a dermatoscope are called dermoscopy images. Currently, most of the computer automated systems use the dermoscopy images for analyzing and diagnosing skin cancer patients. However, these methods are still in their preliminary stage to be used by dermatologists in a clinical environment [2]. In recent years, the use of smartphone cameras to promote health care and assist in early detection of the skin lesions. Various applications in smartphones have potential to use these images for review by a dermatologist or automated detection of the skin lesions [3].

Pre-processing is an important step in every image segmentation technique. Various image processing techniques can be used in the pre-processing stage to help remove redundant data from the input image. Image smoothing and denoising is one of the essential pre-processing methods which is used to remove additive noise from the image that is introduced during the image capturing process. Different linear and non-linear filtering methods to de-noise the images have been suggested. In linear filtering approach, e.g. Averaging, Gaussian filtering etc., every image pixel is assigned a value based on a linear weighted relation with the surrounding pixels. Gaussian filtering uses a Gaussian function to transform the image pixels and smooth the image for segmentation. Most of the linear filtering approaches end up in the removal of the image noise but degrade the edge information as well. Anisotropic Diffusion Filtering (ADF) is a non-linear image smoothing and denoising method in which image quality is not degraded after the removal of noise and edge details are also kept accurately for further processing in the segmentation phase [4-5]. The method ensures the fine details in the image are kept while removing the noise using causality and smoothing parameters.

Image Segmentation is a method used in image processing to partition an image into different regions and extract meaningful information. In dermoscopy images, segmentation can be used to identify the boundary of the skin lesions that may lead to cancer. Various image features are extracted from the segmented image that can be used to classify the image as cancerous or non-cancerous. Several image segmentation techniques can be used to extract the boundary of the skin lesions like thresholding, k-means clustering, and region growing, etc. Thresholding method to segment an image uses a threshold value to convert an image from grayscale into binary. In Otsu's method [6], this threshold value is selected by maximizing the variance of the image. In adaptive thresholding, the threshold value for every pixel of the image is selected based on its surrounding pixel values. This adaptive method can help overcome the varying light conditions in the input image and provides a better conversion from gray-scale image to binary image.

In post-processing, different morphological operations can be applied to extract the foreground data from background pixels. In morphological opening by reconstruction, the background objects are removed using a structuring element and the image is reconstructed. The morphological closing by reconstruction follows this step in which the remaining foreground object is enhanced and any spots left in the image are removed.

In this work, we used ADF in pre-processing stage for smoothing and to enhance the skin lesion then adaptive thresholding is applied to segment the skin lesions, which is also the motivation of this work as these both methods are not used in the skin lesion segmentation. The breakdown of this paper is as follows, section-2 presents the literature review, in section-3 ADF is explained, section-4 and 5 present proposed methodology and experimental results and analysis respectively and paper is concluded in last section.

2. LITERATURE REVIEW

Various methods to automate the segmentation of melanoma skin lesions have been proposed so far, Otsu's method of image thresholding which is based on maximization of image variance is a frequently used method for skin lesion segmentation [6]. In all the fixed thresholding techniques, a cutoff value is selected based on which the image is converted from gray-scale into binary.

The authors in [7] proposed a weighted segmentation method called SWOT for the segmentation of pigmented skin lesions in macroscopic images. The process is a modification of Otsu's thresholding technique by taking regions from different areas of the image and selecting a weighted threshold based on the regions of individual characteristics. They used 152 images from the Alcón et al. data set [8] and 137 images from Dermquest dataset [9]. Their proposed method reduces the average segmentation error (XOR error) by 5% and the average sensitivity by 4.5% in unsupervised segmentation approach.

A dictionary based approach to segment the pigmented melanocytic skin lesions is proposed in [10]. The input images are assumed to be captured by standard cameras having a single skin lesion that is present in the center of the image. The image is converted into three channels which are partitioned into image patches. A dictionary is created for every image patch in an unsupervised manner, and normalized graph cuts are used to segment the image. This method was tested on different data sets and provided an average segmentation error (XOR Error) of around 21% which is quite low compared to various other segmentation methods. This algorithm also obtained a high value of accuracy and specificity when compared with various segmentation techniques.

A combination of Fuzzy C Means (FCM) algorithm, Image thresholding, and level set technique was used for the segmentation of skin lesions in [11]. Three class FCM is applied to the input image and every pixel is assigned to one of the class based on its intensity value. An adaptive thresholding value is calculated using minimum and maximum of each class, and these parameters are used to initialize the Level Set (LS) function in LS evolution. This method achieved an average True Detection rate of 92.6%, False Positive Rate of 4.66%, and False Negative rate of 7.34%. The algorithm also performed better when compared with Fuzzy C Means, Adaptive Thresholding and Region-Based Active Contours methods applied individually.

A histogram based image segmentation approach to detect skin lesions was proposed in [12]. The input image is converted into gray-scale and Weiner filtering method is applied to de-noise the image. Next, histogram-based segmentation is performed by dividing the image based on histogram into two classes and selecting the optimum threshold value. The black spots inside the segmented image are removed in the post-processing stage using morphological operations. Hammoude Distance (HM) and True Detection Rate (TDR) were used to compare the results with various segmentation techniques. The proposed method achieved the HM of 11.37% and maximum TDR of 96.32% when compared with other segmentation methods. Other methods which have been used for the segmentation of skin lesion are Non-negative matrix factorization, Watershed transformation technique with improvement as well and color channel based segmentation in [13-15].

The authors in [16] used Neural Network approach for segmentation of melanoma skin lesions. A segmentation algorithm called Texture Distinctiveness Lesion Segmentation (TDLS) was introduced that used back propagation neural network and texture characteristics of skin lesions to segment the image. The texture distributions of the image are used to calculate the distinctive metrics. A statistical Region Merging (SRM) algorithm is applied to segment the image into different regions based on the texture similarities. Otsu thresholding is then applied to identify the lesion or skin regions in the image. The output of TDLS is supplied to a One-Layer back propagation neural network that increases the accuracy of the segmented image. The TDLS algorithm including neural network is compared with other image segmentation approaches, i.e. L-SRM [17], Otsu-R [18] and Otsu-RGB [19]. The Otsu-R method is similar to Otsu thresholding method but finds the threshold using the red channel of the image whereas the Otsu-RGB method uses all the three channels of the image and finds the threshold for each channel. These methods are used as benchmark techniques for comparison with our proposed methodology.

3. ANISOTROPIC DIFFUSION FILTER

In non-linear filtering methods all the pixels of the image are processed by a similar function which can merge different regions information. In the segmentation of skin cancer, the precise detection of the cancer boundary is extremely important therefore these linear filtering techniques are not preferred. ADF solves this problem by increasing the spatial conduction in more homogeneous regions of the image and avoids major alteration of the signal along region boundaries. ADF carries two main attributes, which includes causality and piecewise smoothing. Causality means no fictitious information should be induced while passing from coarser to finer scale and piecewise smoothing is a process in which intraregional smoothing should occur preferentially as compare to interregional. Both attributes can preserve edges of skin lesion in smoothed image thus improving the process of segmentation [4-5].

The main goal of using ADF is to make diffusion process higher in homogeneous regions and slow down the process where the gradient of the image is higher, which corresponds to the edges of the image. The model can be represented by Equation 1.

$$\frac{\partial I}{\partial t} = div\big(h(|\nabla I(x,y,t)|)\,\nabla I(x,y,t)\big) \quad (1)$$

Where the initial condition is $I(x,y,0) = I_0(x,y)$, for read image I , $\nabla(.)$ and $div(.)$ are gradient and divergence operations respectively. The diffusion operator $h(.)$ holds very important functionality of detecting the edges in an image; usually it is decreasing function also referred as conduction or edge stopping function. Two conduction operators were proposed in [5] as shown in Equation 2-3.

$$h(\nabla I) = exp\left[-\left|\frac{\nabla I}{s}\right|^2\right] \quad (2)$$

$$h(\nabla I) = \frac{1}{1 + \left|\frac{\nabla I}{s}\right|^2} \quad (3)$$

s in conduction operator which controls the threshold value; if $\nabla I < s$ then pixels are considered as part of homogenous or interior region so higher smoothing should be done, if $\nabla I > s$ then pixels are considered to be part of edges so they should be less blurred. In this research, we used the value $s = 1/30$ and conduction operator used is as in Equation 2, because the best results were achieved with these parameters.

Conduction operator s will be applied on each pixel after calculating the difference with respect to its four neighbors in East, West, North and South directions, as shown in Equation 4-7.

$$\nabla_E I_{n,m} = I_{n,m+1} - I_{n,m} \ , \qquad h_{E(n,m)} = h\left|\nabla_E I_{n,m}\right| \quad (4)$$

$$\nabla_W I_{n,m} = I_{n,m-1} - I_{n,m} \ , \qquad h_{W(n,m)} = h\left|\nabla_W I_{n,m}\right| \quad (5)$$

$$\nabla_N I_{n,m} = I_{n-1,m} - I_{n,m} \ , \qquad h_{N(n,m)} = h\left|\nabla_N I_{n,m}\right| \quad (6)$$

$$\nabla_S I_{n,m} = I_{n+1,m} - I_{n,m} \ , \qquad h_{S(n,m)} = h\left|\nabla_S I_{n,m}\right| \quad (7)$$

Where $I_{n,m}$ represents the brightness level of each pixel.

4. PROPOSED METHODOLOGY

Our proposed method is divided in to three main stages. First stage is pre-processing which includes smoothing of skin lesion in image. In the second stage, adaptive thresholding and morphological operations are applied. In the final stage, segmentation is performed.

The process starts by reading the image $I_{n,m}$ then applying gray scale conversion on it. In pre-processing stage, the image will be filtered by ADF, as explained in section-3. A 2-Dimensional Fast Fourier Transform (FFT) is applied over image; which takes the image from the spatial domain in to the frequency domain. The reason to apply FFT is that frequency domain is computationally faster as compare to spatial domain therefore most filtering methods are applied in frequency domain. In frequency domain image is decomposed into its sinusoidal components which makes it easier to target a specific frequency component. FFT is calculated as given in Equation 8.

$$F(x,y) = \sum_{n=0}^{N-1}\sum_{m=0}^{M-1} I(n,m) e^{-2\pi j\left(\frac{xn}{N}+\frac{ym}{M}\right)} \quad (8)$$

Where $I(n,m)$ is the image pixel at position (n,m) and $F(x,y)$ is the frequency component of image at (x,y) , N and M are image dimensions. After FFT the zero frequency component of the image is shifted to the center of the image spectrum, which brings the average brightness values of the image in the center.

In order to focus on the cancerous part of the image, low pass Gaussian filter is applied over the image with cutoff frequency of 40, this will further smooth the image by ignoring pixels which are non-cancerous. Gaussian kernel is shown in Equation 9, which will be convolved with the $F(x,y)$.

$$GF(x,y) = \frac{1}{2\pi\sigma^2} e^{-\frac{x^2+y^2}{2\times\sigma^2}} \quad (9)$$

Where σ is the variance which is set to 40. After convolution, the Inverse FFT will be applied to obtain the filtered image $I_{n,m}$. To ignore the non-affected part of the image, pixel manipulation is applied to the ground pixels. All the pixels having value greater than 155 will be assigned 255 which will turn the non-cancerous part of the image into white.

Sometimes due to non-uniform illumination conditions, image background becomes uneven which can make the segmentation task difficult. Generally adaptive thresholding filtering is used to differentiate the foreground of the image, which is the cancerous part, from the background of the image. It will segment the image by assigning a foreground value to all pixel having intensity less than a threshold and for the rest of the pixels a background value is assigned to secure a binary image. There are several methods to set the threshold value, in our case best result are achieved by using locally derived threshold based on mean [20]. To improve the results, local threshold is assigned values of (Mean-C), where C is a constant. A window $W(x,y)$ is defined and mean is calculated as shown in Equation 10.

$$\mu = \frac{1}{p \times p} \sum_{x=0,y=0}^{x=p,y=p} W(x,y) \quad (10)$$

And local threshold $T = \mu - C$. In our case optimal results were achieved with $C = 0.02$.

Morphological operations like opening, erosion and dilations are applied on binary image to preserve the information of the foreground part of the image, erode and enlarge the boundary of foreground pixels respectively.

In this last part of the algorithm segmentation is applied on basis of boundary conditions. All the foreground parts of the image are referred to as objects. The largest object, which is also referred to as the reference object, is found by calculating the number of black pixel values in all objects and selecting the maximum one, as shown in Equation 11.

$$M_O = Max\left(\sum_{i=1}^{p} O_i(n,m) = 0\right) \quad (11)$$

Where O_i is the number of objects detected in the image having only black pixels and M_o is the selected reference object which has highest number of pixels. Distance of all the objects from reference object is calculated by Equation 12.

$$D_{Oi} = \sqrt{(M_O(n) - O_i(n))^2 + (M_O(m) - O_i(m))^2} \quad (12)$$

If the distance D_{oi} of object O_i from the reference object M_o is greater than 200 pixels than that object is ignored and remaining objects will be considered as the part of the cancer or foreground of the image. Calculate the boundaries of the selected objects and exact segment of the affected part is obtained by mapping it on original image.

5. RESULTS AND ANALYSIS

5.1 Evaluation Statistical Parameters

In order to evaluate the performance of proposed technique, statistical methods based on Dice Similarity Coefficients (DSC), Jaccard Similarity Coefficients (JSC), Sensitivity, Specificity and Accuracy is used. These parameters will evaluate the performance on the basis of number of same pixels identified between ground truth image and image which is segmented by the proposed method. These parameters use the terms True Positive (TP), True Negative (TN), False Positive (FP) and False Negative (FN). These terms are mainly used to analyze the performance of a segmented image. Ground truth image will be a reference image in which the segmented part also referred to as foreground or black pixels and remaining pixels are considered to be the background or white pixels. In this scenario TP is equivalent to number of pixels correctly segmented as foreground, TN is the number of pixels segmented correctly as background, FP is

number of pixels segmented falsely as foreground and FN is equivalent to number of pixels falsely segmented as background.

DSC is a validation metric which will measure the percentage of overlapped segmented parts of any two images in spatial domain [21]. JSC will also measure the similarity between two segmented images by calculating the size of the intersection of similar segmented part of the image divided by the union of it [22]. DSC and JSC are calculated by the following Equations 13-14.

$$D(G,I) = \frac{2(G \cap I)}{(G + I)} = \frac{2 \times TP}{((FP + TP) + (TP + FN))} \quad (13)$$

$$J(G,I) = \frac{(G \cap I)}{(G \cup I)} = \frac{TP}{FP + TP + FN} \quad (14)$$

Where G and I represent the pixels belongs to segmented foreground of ground truth image and proposed method image respectively, $\cap$ and $\cup$ is logical AND and OR operators respectively.

Sensitivity shows the performance of an algorithm on basis of number of TP pixels identified, which is similar to the correct estimation of the foreground of the image. Specificity is equivalent to performance measurement based on correct estimation of TN pixels, which is similar to the percentage of the correct estimation for background of the image. Accuracy is the calculation of overall correct estimation of both TP and TN pixels, which means it will calculate the percentage of overall correct segmentation of both foreground and background of the image [22]. Sensitivity, specificity and accuracy is calculated as shown in Equation 15-17.

$$Sensitivity = \frac{TP}{TP + FN} \quad (15)$$

$$Specificity = \frac{TN}{TN + FP} \quad (16)$$

$$Accuracy = \frac{TP + TN}{TP + TN + FP + FN} \quad (17)$$

5.2 Experimental Results

The images used in this research are taken from International Skin Imaging Collaboration (ISIC) archive [23]. Images in this database includes cancer types like benign and malignant melanocytes, nevi and basal cell carcinomas, Seborrheic keratosis etc. which are confirmed by biopsy. From this data set we have used 300 images with different skin cancer history, phototype, size, subtypes, localization and patient age. The ground truth segmented images are also provided in this data set.

Visual results for five selected samples are presented in Figure 1, the selection of these samples is done on the basis of different characteristics of image quality and skin lesion, which is the cancerous part in the image. Sample-1 shows the benign malignant which is localized at the abdomen, it has uniform lesion for cancerous part. In sample-4 dysplastic nevus was diagnosed and localized at the upper limb, it has uniform lesion only at the boundary of the foreground of image. Sample-3 also diagnosed dysplstic nevus but localized at the breast and it has a non-uniform lesion as the right side of the foreground of the image is more affected as compare to left side, as shown in Figure 1(a). In sample-2 melanoma was diagnosed and located at the pubis, this image has bad illumination due to poor quality of image as it is dark at the corners, as shown in Figure 1(a), also skin lesion in this sample is covered by body hair. Sample-5 is diagnosed as benign malignant and located at the upper extremities of body, it has rough skin lesion with degraded image resolution and illumination. The statistical results for sample images are presented in Table 1.

The proposed method segmented all the sample images similar to the ground truth images, except for sample-3, in which only right side of the lesion is segmented, shown in Figure 1(f). In this sample image, the left part of the lesion was ignored due to pixel manipulation, same can be verified from statistical analysis in Table 1, the JSC and sensitivity are 75.6% and 75.5% respectively and overall accuracy is also the lowest which is 94.3% as compared to other sample images. Sample-1 and 4 secured the highest accuracy as the skin lesion was uniform and image quality was better therefore segmented part is almost similar to ground truth image and secured highest DSC, JSC and accuracy, as shown in Table 1. In sample-2, skin lesion was under body hair and due to bad illumination there were black spots in the image corners but this proposed technique even segmented this image with accuracy of 95.2%. This proposed technique ignored the hair and other objects in image by boundary condition implementation, as shown in Figure 1(e), because the distance of these objects from skin lesion was more than 200 pixels, distance measurement can be seen by blue lines in Figure 1(e) for sampe-2. For sample-5, the image quality and resolution was degraded but due to ADF and Gaussian filtering, a better image is restored for segmentation, shown in Figure 1(b). Non skin lesion parts at the corner of this sample image is ignored by same boundary condition, as shown in Figure 1(e). Inner portion of skin lesion for sample-2 and 5 got ignored due to morphological functions and adaptive thresholding but it did not affect the overall segmentation results due to efficient boundary condition implementation as given in Equation 11 and 12 of the proposed methodology. Overall it can be stated that the proposed methodology performed better segmentation for all conditions except when skin lesion is non-uniform at the boundaries and this method ignored the less affected part of the skin lesion.

The averaged statistical results for 300 images are presented in Table 2. In this table the performance of the proposed method is also compared with averaged results of other techniques like L-SRM [17], Otsu-R [18], Otsu-RGB [19] and TDLS [13]; comparison is done on basis of sensitivity, specificity and accuracy only as results for DSC and JSC were not available for benchmark techniques. The proposed method achieved the highest specificity and accuracy. As for sensitivity, the proposed method is at third place as shown in Table 2. The main reason for lesser sensitivity is due to images which have higher no-uniformity in skin lesion and same was observed in visual and statistical analysis of sample-3 in Figure 1 and Table 1 respectively.

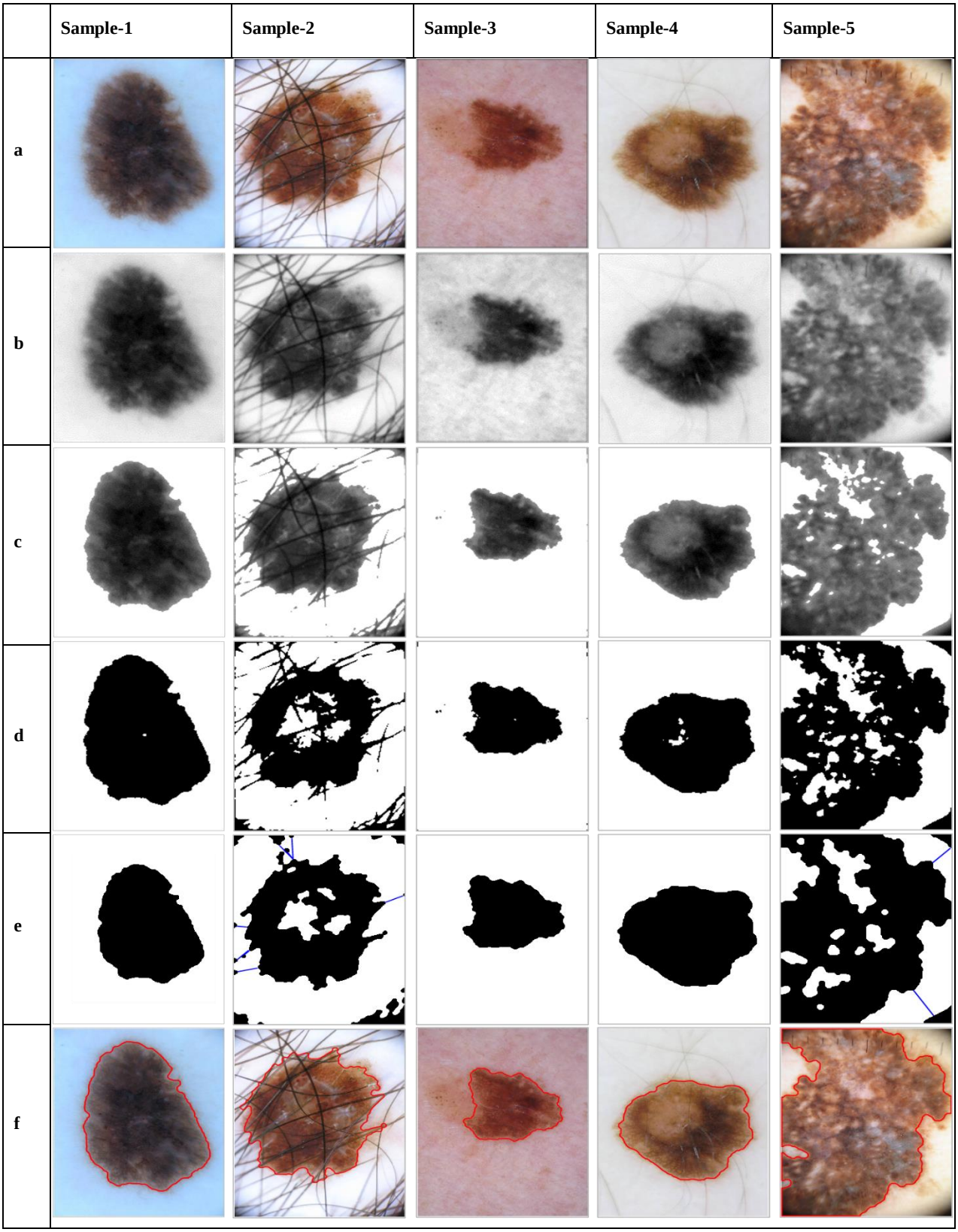

Figure 1. : Five samples of segmented images by proposed technique, (a) Original Image, (b) Gaussian filtered image, (c) Image after ground pixel manipulation, (d) Image after adaptive thresholding, (e) Image after morphological operations and boundary conditions, (f) Final segmented image.

Table 1. Statistical results for sampled images

	DSC	JSC	Sensitivity	Specificity	Accuracy
Sample-1	98.3%	96.6%	96.9%	99.8%	98.9%
Sample-2	92.0%	85.3%	95.0%	95.3%	95.2%
Sample-3	86.1%	75.6%	75.5%	98.7%	94.3%
Sample-4	98.5%	97.1%	99.8%	99.0%	99.2%
Sample-5	85.2%	74.1%	92.8%	94.8%	94.9%

Table 2. Averaged statistical results for all 300 images for proposed method and benchmark techniques

	Sensitivity	Specificity	Accuracy	DSC	JSC
Proposed Method	88.4%	99.4%	96.6%	91.56%	84.97%
L_SRM	89.4%	92.7%	92.3%	--	--
Otsu-R	87.3%	85.4%	84.9%	--	--
Otsu-RGB	93.6%	80.3%	80.2%	--	--
TDLS	88.8%	98.0%	96.0%	--	--

6. CONCLUSION

In this paper, we presented a novel and simple methodology to segment the skin lesion in which ADF is used initially to secure clean skin lesion in the image, then binary image is generated by adaptive thresholding and final segmented image is obtained by boundary conditions. The proposed methodology tested over 300 images taken from ISIC archive and averaged results based on statistical parameters are presented and compared with existing techniques. The proposed method achieved higher accuracy as compared to benchmark techniques. Visual results based on different skin lesions are also presented here in which higher accuracy of segmentation for the proposed method can be observed. However, a degraded segmentation performance of the proposed technique is observed if skin lesion is non-uniform on the edges. This issue can be solved by increasing the limit in pixel manipulation step which can affect other constraints in segmentation hence this issue can be addressed in further research work.

7. REFERENCES

[1] Korotkov, K. and Garcia, R., 2012. Computerized analysis of pigmented skin lesions: a review. *Artificial intelligence in medicine*, *56*(2), pp.69-90.

[2] Perrinaud, A., Gaide, O., French, L.E., Saurat, J.H., Marghoob, A.A. and Braun, R.P., 2007. Can automated dermoscopy image analysis instruments provide added benefit for the dermatologist? A study comparing the results of three systems. *British Journal of Dermatology*, *157*(5), pp.926-933.

[3] Kassianos, A.P., Emery, J.D., Murchie, P. and Walter, F.M., 2015. Smartphone applications for melanoma detection by community, patient and generalist clinician users: a review. *British Journal of Dermatology*, *172*(6), pp.1507-1518.

[4] Perona, P. and Malik, J., 1990. Scale-space and edge detection using anisotropic diffusion. *IEEE Transactions on pattern analysis and machine intelligence*, *12*(7), pp.629-639.

[5] Jaffar, M.A., Zia, S., Latif, G., Mirza, A.M., Mehmood, I., Ejaz, N. and Baik, S.W., 2012. Anisotropic diffusion based brain MRI segmentation and 3D reconstruction. *International Journal of Computational Intelligence Systems*, *5*(3), pp.494-504.

[6] Otsu, N., 1979. A threshold selection method from gray-level histograms. *IEEE transactions on systems, man, and cybernetics*, *9*(1), pp.62-66.

[7] Zortea, M., Flores, E. and Scharcanski, J., 2017. A simple weighted thresholding method for the segmentation of pigmented skin lesions in macroscopic images. *Pattern Recognition*, *64*, pp.92-104.

[8] Alcón, J.F., Ciuhu, C., Ten Kate, W., Heinrich, A., Uzunbajakava, N., Krekels, G., Siem, D. and De Haan, G., 2009. Automatic imaging system with decision support for inspection of pigmented skin lesions and melanoma diagnosis. *IEEE journal of selected topics in signal processing*, *3*(1), pp.14-25.

[9] Amelard, R., Wong, A. and Clausi, D.A., 2012, May. Extracting high-level intuitive features (HLIF) for classifying skin lesions using standard camera images. In *Computer and Robot Vision (CRV), 2012 Ninth Conference on* (pp. 396-403). IEEE. Data Set: http://vip.uwaterloo.ca/demos/skin-cancerdetection

[10] Flores, E.S. and Scharcanski, J., 2014, August. Segmentation of pigmented melanocytic skin lesions based on learned dictionaries and normalized graph cuts. In *Graphics, Patterns and Images (SIBGRAPI), 2014 27th SIBGRAPI Conference on* (pp. 33-40). IEEE.

[11] Masood, A. and Al-Jumaily, A.A., 2013. Fuzzy C mean thresholding based level set for automated segmentation of skin lesions. *Journal of Signal and Information Processing*, *4*(03), p.66.

[12] El Abbadi, N.K. and Miry, A.H., 2014. Automatic segmentation of skin lesions using histogram thresholding.

[13] Cavalcanti, P.G., Scharcanski, J., Martinez, C.E. and Di Persia, L.E., 2014, May. Segmentation of pigmented skin lesions using non-negative matrix factorization.

In *Instrumentation and Measurement Technology Conference (I2MTC) Proceedings, 2014 IEEE International* (pp. 72-75). IEEE.

[14] Grau, V., Mewes, A.U.J., Alcaniz, M., Kikinis, R. and Warfield, S.K., 2004. Improved watershed transform for medical image segmentation using prior information. *IEEE transactions on medical imaging*, *23*(4), pp.447-458.

[15] Sagar, C. and Saini, L.M., 2016, July. Color channel based segmentation of skin lesion from clinical images for the detection of melanoma. In *Power Electronics, Intelligent Control and Energy Systems (ICPEICES), IEEE International Conference on* (pp. 1-5). IEEE.

[16] John, J.M., Samuel, S.S. and John, N.M., 2014. Segmentation of skin lesions from digital images using texture distinctiveness with neural network. *International Journal of Advanced Research in Computer and Communication Engineering*, *3*(8), pp.7777-7780.

[17] Emre Celebi, M., Kingravi, H.A., Iyatomi, H., Alp Aslandogan, Y., Stoecker, W.V., Moss, R.H., Malters, J.M., Grichnik, J.M., Marghoob, A.A., Rabinovitz, H.S. and Menzies, S.W., 2008. Border detection in dermoscopy images using statistical region merging. *Skin Research and Technology*, *14*(3), pp.347-353.

[18] Cavalcanti, P.G., Scharcanski, J. and Lopes, C.B., 2010, November. Shading attenuation in human skin color images. In *International Symposium on Visual Computing* (pp. 190-198). Springer, Berlin, Heidelberg.

[19] Cavalcanti, P.G. and Scharcanski, J., 2011. Automated prescreening of pigmented skin lesions using standard cameras. *Computerized Medical Imaging and Graphics*, *35*(6), pp.481-491.

[20] Ahmad, M.B. and Choi, T.S., 1999. Local threshold and boolean function based edge detection. *IEEE Transactions on Consumer Electronics*, *45*(3), pp.674-679.

[21] Dice, L.R., 1945. Measures of the amount of ecologic association between species. *Ecology*, *26*(3), pp.297-302.

[22] Balafar, M.A., 2014. Gaussian mixture model based segmentation methods for brain MRI images. *Artificial Intelligence Review*, *41*(3), pp.429-439.

[23] The International Skin Imaging Collaboration: https://isic-archive.com/

Authors' background

Your Name	Title*	Research Field	Personal website
Adil H. Khan	PhD Scholar/Lecturer	Medical Image Processing	
Ghazanfar Latif	PhD Scholar/Lecturer	Machine Learning, Image Processing	
D.N.F. Awang Iskandar	Senior Lecturer	Medical Image Processing	
Jaafar Alghazo	Assistant Professor	Machine Learning, CAD Systems	
Mohsin Butt	Lecturer/ PhD Scholar	Medical Image Processing	